

1-MeV ELECTROSTATIC ION ENERGY ANALYZER*

F.M. Bieniosek[#] and M. Leitner, LBNL, Berkeley CA 94720, U.S.A.

Abstract

We describe a high-resolution 90-degree cylindrical electrostatic energy analyzer for 1-MeV (singly ionized) heavy ions for experiments in the Heavy Ion Fusion Science Virtual National Laboratory (HIFS-VNL). By adding a stripping cell, the energy reach of the analyzer can be extended to 2 MeV. This analyzer has high dispersion in a first-order focus with bipolar deflection-plate voltages in the range of ± 50 kV. We present calculations of vacuum-field beam trajectories, space-charge effects, field errors, and a multipole corrector. The corrector consists of 12 rods arranged in a circle around the beam.

The improved energy diagnostic will allow measurements of beam energy spread, such as caused by charge exchange or temperature anisotropy, and better understanding of experimental results in planned longitudinal beam studies. Examples for such experiments include investigations of a beam patching pulser to correct errors in the head and tail of the transported beam bunch, and energy errors derived from ripples in the injector voltage waveform.

INTRODUCTION

With the development of optical diagnostic techniques in the heavy-ion fusion program, we have gained the ability to measure all four transverse dimensions of the beam distribution [1]. However, in order to characterize the beam longitudinally, information on the beam particle energy distribution and the beam energy must be obtained. Beam energy could previously be measured with existing energy analyzers and time-of-flight techniques at relatively low resolution and accuracy. For instance, in recent measurements on HCX [2] the analyzer's measured energy distribution width was $\sigma(E)/E \sim 0.5\%$, which was inadequate to measure at the desired resolution of approaching 10^{-4} .

ENERGY ANALYZER DESIGN

The electrostatic energy analyzer (EEA) is a 90° cylindrical sector field analyzer with first-order focus [3, 4]. The EEA has a radius of curvature of 50 cm, a separation between plates of 2.5 cm. The deflection plate voltages to provide the 90° sector bend field for a 1-MeV ion beam are ± 50 kV for K^+ and ± 25 kV for K^{++} .

*Work performed under the auspices of the U.S. Department of Energy by the university of California, Lawrence Berkeley National Laboratory under Contract No. DE-AC03-76F00098.

[#]fmbieniosek@lbl.gov

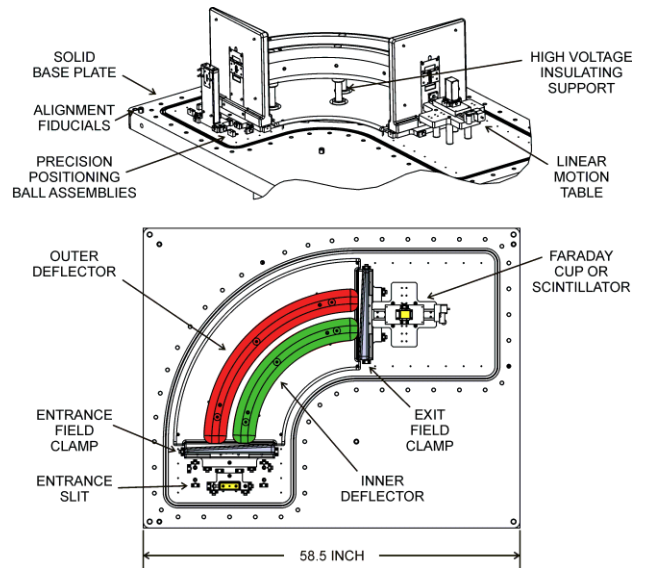


Fig. 1. Mechanical Design of the High Resolution Energy Analyzer.

For the design and construction of the EEA careful attention was paid to mechanical tolerances, equipment calibration, highly-stable high voltage supplies, and issues such as fringe fields, beam collimation, beam space-charge effects, and beam/plasma loading of the deflector plates. Each of these topics are discussed briefly in the following sections.

As shown in figure 1 the EEA consists of: (1) An entrance slit, which determines the object size. (2) An

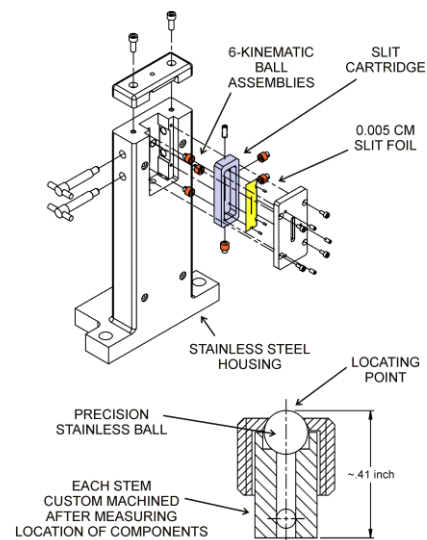


Fig. 2. Example for the precision-machined kinematic supports used throughout the EEA assembly to reach better than 0.005 cm component alignment.

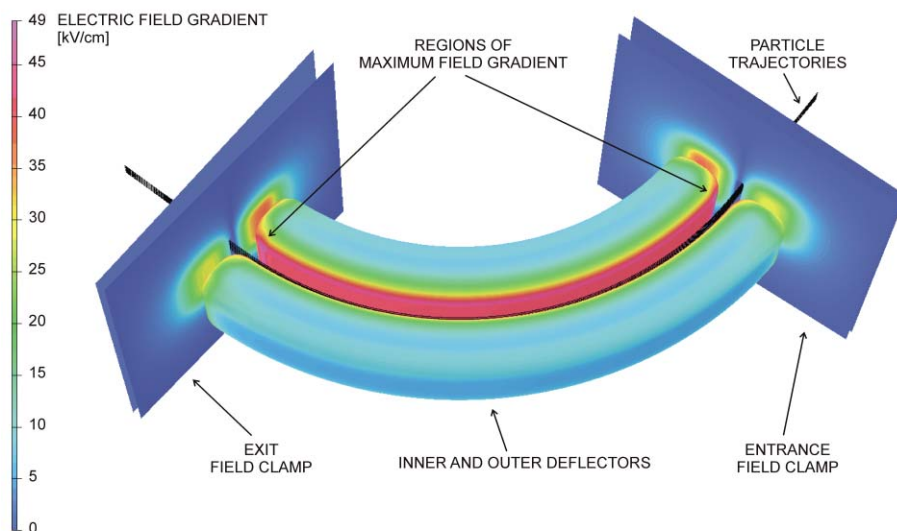


Fig. 3. Opera-3D electric field calculation including particle trajectories. The maximum field gradient for 1 MeV operation is less than 50 kV/cm.

entrance field clamp, which limits the beam divergence by collimating the ion beam in addition to shaping the deflector entrance electric field. According to [5] the field clamps are angled with respect to the deflectors to establish a radially decreasing electric field equivalent to that between the deflectors. (3) The main deflectors. (4) An exit field clamp. (5) A Faraday cup with exit slits or a scintillator mounted on a vacuum linear stage. The linear stage allows fine tuning to move the beam diagnostics into the analyzer focal point.

Mechanical Design: Each component of the EEA including the heavy deflectors have been mounted on kinematic supports consisting of six sphere assemblies. As example, the entrance slit assembly is shown in figure 2. The base of the sphere assemblies are custom machined to move the components to their theoretical exact locations within 0.002 inches. The alignment of the large EEA components has been verified on a computer measuring machine (CMM). In order to provide a large thermal mass and to match thermal expansion for temperature stability all components have been machined out of stainless steel. The 3" thick, 58.5" x 46.5" base plate as well as the large deflectors are machined out of solid stainless steel.

Beam Collimation: The theoretical energy resolution Δ of the EEA is determined [5] by the ratio of the entrance and exit slit widths w to the radius of curvature ρ : $\Delta=w/\rho$. The entrance and exit slits are positioned at the first-order focal points of the EEA [5], 17.5 cm from the theoretical hard edge field boundary of the 90-degree bend. With a narrow entrance slit of .005 cm, and a similar-sized detector slit, or by replacing the detector with a scintillator-based optical beam detection system, we can expect a resolution of a few $\times 10^{-4}$ in a practical analyzer system with a 50-cm radius of curvature.

The divergence of the incoming ion beam causes a focusing error s_e that is second order in entrance angle

α of the analyzed particle with respect to the centerline. Focusing error is similar to that for the 127-degree analyzer [4]: $s_e = 4\alpha^2 r_0 / 3$, where r_0 is the radius of curvature of the analyzer. Therefore, the entrance angle must be limited to less than ± 10 mrad to maintain the intrinsic error $s_e < 1 \times 10^{-4}$. This criterion has been met by the entrance slit and an additional slit ($w=0.273$ cm, $dist=14$ cm after the entrance slit) in the entrance field clamp.

Simulation: The EEA has been modeled using the finite element code Opera-3D (see figure 3). The same code was used to trace particles through the actual field geometry, and to verify the design parameters. The effective field length including the fringe fields of the analyzer has been designed to match the integrated field strength of an ideal hard-edge 90 degree sector. In addition, the simulations have been used to determine the good field region in

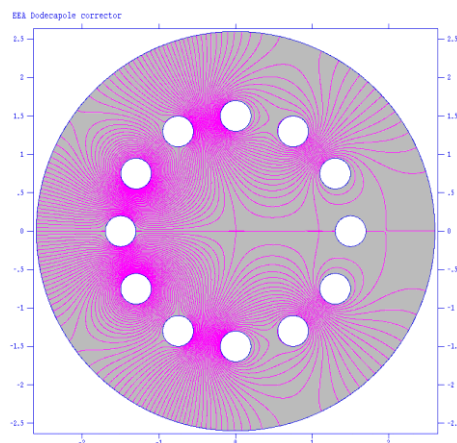


Fig. 4. Field structure in a dodecapole corrector, with the rod voltages distributed to provide a combination of a quadrupole and a sextupole field.

between the deflectors. The deflectors are 13 cm high. For high-resolution operation the maximum vertical beam size inside the deflectors has been constrained to 1.3 cm by limiting the entrance slit's and entrance field clamp's aperture height to .5 cm and .77 cm respectively.

Higher Order Correction: To ensure sufficient flexibility to meet the desired level of resolution with real-world alignment and calibration tolerances, a dodecapole [7, 8] corrector may be placed in the drift space between the entrance slit of the EEA and the main deflection plates. The corrector consists of 12 circular rods arranged in a circle around the beam. A dodecapole arrangement of electrodes has excellent and flexible properties as an electrostatic einzel lens, dipole, quadrupole, sextupole, or a linear combination of these, depending on the voltage distribution applied to the rods. A conceptual drawing of the multipole corrector is presented in Figure 4. It shows the electrostatic field structure for a combination quadrupole and sextupole field. The quadrupole and sextupole fields correct first order alignment errors and second order image distortions, respectively. We expect to be able to correct these errors and distortions of the beam images at the detector plane into the 10^{-4} range. We do not expect to require higher order field corrections than sextupole.

Non-Isochronous Characteristic: The EEA is not isochronous with respect to particle injection angle. Using the orbit equation for a particle at the design energy

$$\phi = \int_1^y [2\sec^2 \alpha \log y - y^2 + \sec^2 \alpha]^{-1/2} dy$$

where $y = \rho_0/\rho$, ρ is the particle radius, and ϕ is the angle with respect to the origin of the radial electric field E [4], the time of flight is estimated from the path length under the assumption of circular motion by $mv^2/\rho = eE$, or $v = \sqrt{V_0 \rho_0 / m \rho}$ where V_0 is the design particle energy and m is the particle mass. For example, the relative transit time through the analyzer varies by $\pm 1.2\%$ for an injection angle variation of ± 10 mrad. This corresponds to a time variation of about ± 9 ns for a 1-MeV K^+ ion beam. This non-isochronicity limits the time resolution of the diagnostic.

Space Charge Influence: Space charge limits the amount of charge that can be injected into the EEA. Consider the envelope equation $x'' = k_e x + \frac{\epsilon_x^2}{x^3} + \frac{2Q}{x+y}$ where the first

term represents the external focusing field, the second term is the emittance term, and the third term is the space charge term. Here Q is the dimensionless perveance

$$Q = \frac{I}{4\pi\epsilon_0 V_0^{3/2} \sqrt{2e/m}}$$

where I is the beam current. In a

sheet beam $y \gg x$ the space charge contribution to the transverse beam dimension x is independent of path length z and thus separable. For path length d the space charge contribution to x is $x = \frac{Qd^2 s}{2r_{beam}^2}$ where s is the slit

width and $r_{beam}^2 = r_{bx} r_{by}$ represents the mean beam radius. Transportable beam current is proportional to $V^{3/2}$ and $m^{-1/2}$. Assuming a minimum detectable beam current, space charge provides a practical lower limit of operation. To maintain spreading of the focal spot $x/s < 1$, the lower limit for K^+ beam energy is roughly 100 keV ($I \sim 5 \mu A$).

APPLICATIONS

1. Neutralized drift compression is crucial to the application of HIFS-VNL ion beams to high energy density physics experiments. The amount of compression achievable depends ultimately on the longitudinal beam energy spread. The EEA will allow accurate measurement of the longitudinal beam energy distribution. For example at a beam energy of 1 MeV, the analyzer with energy resolution $\Delta < 10^{-3}$ should resolve longitudinal beam temperature to accuracy < 0.1 eV [9].
2. Sensitive measurement of beam energy spreading at the injector, for example due to charge exchange or the temperature anisotropy instability, also require a high resolution diagnostic.
3. The EEA will allow improved understanding of longitudinal wave experiments, experiments on the effect of beam patching pulser to correct errors in the head and tail of the beam, and measurements of beam energy errors derived from ripples in the injector voltage waveform. An example of energy measurements using the EEA is shown in Ref. 9.

REFERENCES

- [1] F.M. Bieniosek, et. al. Nucl. Instrum. Methods Phys. Res. A544 (2005) 268-276.
- [2] L. Prost, et. al., Phys. Rev. Spec. Top. – AB 8, (2005) 020101.
- [3] R.E. Warren, J.L. Powell, R.G. Herb, Rev. Sci. Instrum, 18, 559 (1947).
- [4] L. Hughes, V. Rojansky, Phys. Rev. 34, (1929) 284.
- [5] H. Wollnik, Optics of Charged Particles, 1987
- [6] K. Jost, J. Phys. E: Sci. Instrum. 12 (1979) 1001-1005.
- [7] A.J.H. Boerboom, Nucl. Instrum. Methods Phys. Res. A258 (1987) 426-430.
- [8] A.J.H. Boerboom, Int. J. Mass Spect. Ion Proc. 146/147 (1995) 131-138.
- [9] M. Reiser, Theory and Design of Charged Particle Beams, Wiley, 1994, p. 397.
- [10] P.K. Roy, et.al., Phys. Rev. Spec. Top. – AB 9, (2006) 0704